Katayama et al. Progress in Earth and Planetary Science (2015) 2:30
DOI 10.1186/s40645-015-0063-4

Progress in Earth and Planetary Science
a SpringerOpen Journal

RESEARCH Open Access

Can clay minerals account for the behavior of non-asperity on the subducting plate interface?

Ikuo Katayama[1*], Tatsuro Kubo[1], Hiroshi Sakuma[2] and Kenji Kawai[3]

Abstract

Seismicity along the subducting plate interface shows regional variation, which has been explained by the seismic asperity model where large earthquakes occur at strongly coupled patches that are surrounded by weakly coupled regions. This suggests that the subduction plate interface is heterogeneous in terms of frictional properties; however, the mechanism producing the difference between strong and weak couplings remains poorly understood. Here, we propose that the heterogeneity of the fluid pathway and of the spatial distribution of clay minerals plays a key role in the formation of non-asperity at the subducting plate interface. We use laboratory measurements of frictional properties to show that clay minerals on a simulated fault interface are characterized by weak and slow recovery, whereas other materials such as quartz show relatively quick recovery and thereby strong coupling on the fault surface. Aqueous fluids change the mineralogy at the plate interface by producing clay minerals due to hydrate reactions, suggesting that the hydrated weakly coupled regions act as a non-asperity and form a barrier to rupture propagation along the plate boundary at the depths of seismogenic zone.

Keywords: Frictional healing; Clay minerals; Seismic asperity; Subducting plate interface

Background

A plate-boundary earthquake at a subduction zone represents the slip between the subducting and overriding plates, and therefore, differences in the level of seismicity can be attributed to differences in the strength of mechanical coupling at the subducting plate interface (Kanamori 1986). Strongly coupled regions are termed asperity, which ultimately released seismic energy through large megathrust earthquakes due to slip concentration, whereas the weakly coupled regions are known as non-asperity and show slow and continuous slip (e.g., Lay et al. 1981; Beroza and Ide 2011). This asperity model suggests that the subduction plate interface is heterogeneous in terms of the strength of mechanical coupling; however, the mechanism that generates the spatial difference between strong and weak couplings remains unclear.

Laboratory experiments have shown that the frictional strength of fault materials under stationary contact increases with holding time, and this healing process is likely to make an important contribution to the recovery of fault strength during the period between successive seismic cycles (e.g., Marone 1998; Beeler et al. 2001). This recovery process could be different in fault materials, such as reported for the San Andreas Fault, which shows weak or no frictional healing due to the presence of clay minerals, resulting in the mechanical weakness of this active tectonic fault (Carpenter et al. 2011). The alteration of materials at the plate interface by aqueous fluids could form clay minerals, which could in turn contribute to a weakening of the mechanical coupling at the subducting plate interface. To test this hypothesis, we systematically measured the frictional healing of clay minerals in the presence of water, on which basis we examine whether the frictional properties of clays can account for the weakly coupled regions at the subducting plate interface.

Methods

Experimental samples

Chlorite and saponite are common alternation products of basaltic rocks (e.g., Kameda et al. 2011), and illite is

* Correspondence: katayama@hiroshima-u.ac.jp
[1]Department of Earth and Planetary Systems Science, Hiroshima University, Higashihiroshima 739-8526, Japan
Full list of author information is available at the end of the article

frequently recognized in the pelagic sediments that cover oceanic crust (e.g., Underwood 2007). We therefore used these clay minerals for frictional experiments to examine time-dependent frictional healing. Rochester shale was used as the illite-rich simulated gouge. This shale contains 60 % illite, 9 % kaolinite, 20 % quartz, and minor plagioclase (Saffer and Marone 2003). The saponite and chlorite samples are monomineralic. The saponite samples were synthesized by Kunimine Industries, Japan, and the chlorite samples were collected as clinochlore megacryst from the Korshunovskoe mine, Russia. We also tested quartz powder for comparison with the clay minerals. Illite and chlorite were prepared by crushing in a disk mill to produce powders with grain size <75 μm. These powders, along with the original powders of saponite and quartz with grain <50 μm, were used for the friction experiments. These samples were kept in a desiccator at 70 °C for 48 h before experiments. Each of the powdered materials (2.0–2.5 g) was sandwiched between blocks; the thickness of the simulated gouge layer was approximately 0.5 mm in each experiment.

Experimental procedure

We conducted a series of slide-hold-slide frictional experiments using a biaxial frictional testing machine at Hiroshima University, Japan. The powdered samples were placed on the simulated fault surface between gabbro blocks, and two side blocks and central block were placed together to produce a double-direct shear configuration (Additional file 1: Figure S1). A normal stress of 15 MPa was applied via a hydraulic press on the side blocks, and then shear stress was applied by advancing the central block downward at a constant velocity of 3 μm/s. Similar experiments were reported for serpentine gouge in Katayama et al. (2013). The electromagnetic transducer monitored axial displacement, which was corrected by the machine stiffness (4.4×10^8 N/m). The total axial displacement was limited to 20 mm in our assembly (Additional file 1: Figure S1), and we usually started the slide-hold-slide test after 10 mm displacement achieving the steady-state friction. Mechanical data were recorded by data logger (KYOWA EDX-100A) with a sampling rate of 10 Hz. The friction coefficient was calculated from the shear stress divided by the normal stress, assuming zero cohesion. In addition to dry conditions, we performed frictional experiments under wet environments using a water tank to assess the effect of water on frictional healing, where water chemistry was controlled by pure (distilled) water or 0.5 mol/L NaCl solution.

In the experiments, the axial loading was interrupted for periods ranging from 10 to 3000 s after steady-state friction, and we measured the difference between the steady-state friction and the peak friction after each holding period. Friction under stationary contact is known to increase with the logarithm of time as follows: $\mu(t) = \mu_0 + b \log(t)$, where μ_0 is the friction at the beginning of stationary contact, t is holding time, and b is the healing rate (Marone 1998).

Results

Friction coefficient

The experimental results show that the friction coefficient increases with displacement and attains a steady-state level after few millimeters of displacement (Fig. 1). The steady-state friction coefficient shows systematic differences between the studied minerals: 0.65 for quartz, 0.61 for illite, 0.75 for saponite, and 0.39 for chlorite under dry conditions and 0.64 for quartz, 0.41 for illite, 0.09 for saponite, and 0.18 for chlorite under wet conditions (Table 1). The substantial reduction in the friction coefficient of clay minerals in the presence of water is consistent with the results of previous experiments reported by Morrow et al. (2000), in which adsorbed or interlayer water strongly influences the frictional strength of phyllosilicates. Moreover, a first principle calculation suggests that adsorbed water molecules on clay minerals prevents direct contact between mineral surfaces, which results in a substantial reduction in friction coefficient (Sakuma 2013). Water chemistry has only a minor influence on the frictional properties (Table 1), and therefore, the discussion below focuses mainly on the results for wet experiments using pure water.

Frictional healing

After achieving steady-state friction, the axial loading was stopped in each case and held for a period to analyze the effect of frictional healing. Figure 2 shows an example of slide-hold-slide test for illite under wet condition. Friction coefficient decays from the steady-state level during a holding period due to stress relaxation. A peak friction appears when the piston was advanced, and then, it decays to the steady-state friction. The frictional healing, $\Delta\mu$, is calculated as the difference between the peak and steady-state frictions after each holding period. The results for wet conditions show that the frictional healing of clay minerals increases slightly with holding time (Fig. 3), but the rate of strength recovery is substantially lower than that of quartz at same conditions. Figure 4 shows the experimental results for frictional healing, and the results were summarized in Table 1. The quartz gouge shows a high healing rate, $b = 0.014$, which means a relatively quick recovery of fault strength, whereas clay minerals show low healing rate, $b = 0.001–0.004$, suggesting a slow recovery of fault strength. Illite shows a slightly higher healing rate than the other clay minerals probably because of the mixture of quartz in the Rochester shale. Under dry conditions, the healing rate is slightly suppressed, but the clay minerals show a significantly slower strength recovery than quartz, similar to the pattern observed for the wet experiments.

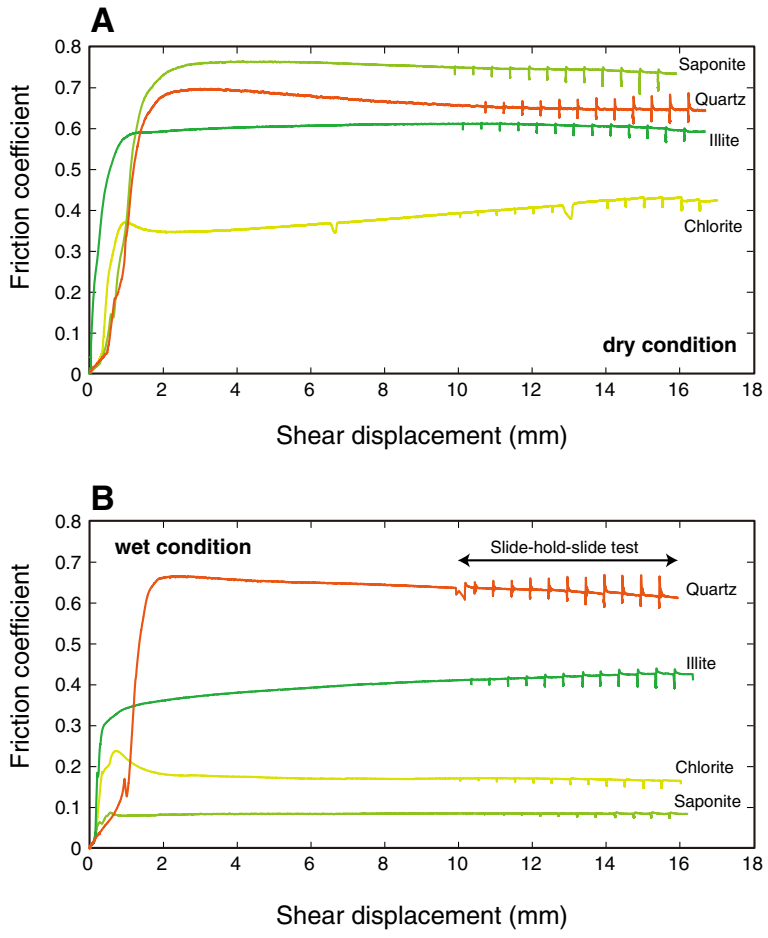

Fig. 1 Experimental results for illite, saponite, chlorite, and quartz under dry (**a**) and wet conditions using distilled pure water (**b**), showing friction coefficient as a function of shear displacement. The friction coefficient differs systematically between minerals, and clay minerals show a significant reduction of friction coefficients under wet condition. Slide-hold-slide tests were performed after reaching a steady-state friction at ~10 mm displacement

Table 1 Condition and result of frictional experiments

Run no.	Material	Dry or wet	Normal stress (MPa)	Loading velocity (μm/s)	Steady-state friction	Healing rate
HTB156	Quartz	Dry	15	3	0.65	0.012
HTB284	Quartz	Wet (pure water)	15	3	0.64	0.014
HTB295	Quartz	Wet (0.5 M NaCl)	15	3	0.62	0.016
HTB273	Illite	Dry	15	3	0.61	0.002
HTB283	Illite	Wet (pure water)	15	3	0.41	0.004
HTB287	Illite	Wet (0.5 M NaCl)	15	3	0.43	0.005
HTB229	Saponite	Dry	15	3	0.75	0.003
HTB279	Saponite	Wet (pure water)	15	3	0.09	0.001
HTB289	Saponite	Wet (0.5 M NaCl)	15	3	0.09	0.002
HTB234	Chlorite	Dry	15	3	0.39	0.001
HTB286	Chlorite	Wet (pure water)	15	3	0.18	0.001
HTB294	Chlorite	Wet (0.5 M NaCl)	15	3	0.16	0.001

Steady-state friction is data observed at 10 mm shear displacement

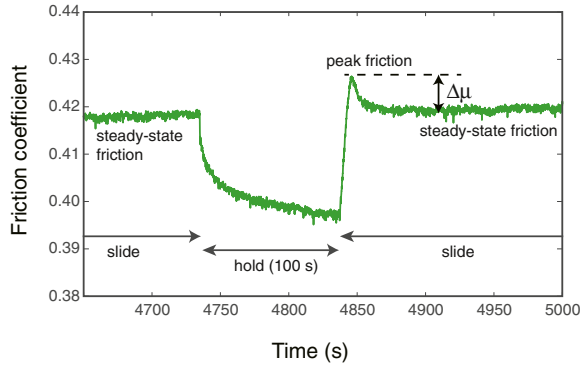

Fig. 2 An example of slide-hold-slide test showing friction coefficient as a function of time for illite under wet condition. Friction coefficient decays from the steady-state level during holding period. When the piston was advanced again (sliding), a peak friction appears, and then friction decays to the steady-state level. The frictional healing ($\Delta\mu$) is difference between the peak and steady-state frictions

After each holding period, the peak friction decayed to the steady-state friction when the axial piston was advanced. Quartz displays oscillatory and transient variation in frictional behavior at times after the peak friction has been attained, whereas the experiments on clay minerals show a continuous decay from peak friction to the steady-state value (Fig. 3). The transient distance from the peak to steady-state friction seems to be systematically different between quartz and clay minerals, in which clay minerals tend to exhibit a large slip-weakening distance.

Discussion

Mechanism of frictional healing of clay minerals

Our experiments indicate that frictional healing varies with mineralogy in the simulated faults. In particular, clay minerals are characterized by a low healing rate. Similar weak healing has been reported in clay-rich natural fault materials from the San Andreas Fault (Carpenter et al. 2011) and from the Zuccale Fault in central Italy (Tesei et al. 2012). Serpentines, the products of mantle hydration, have also been reported to exhibit a low healing rate and large slip-weakening distance (Katayama et al. 2013).

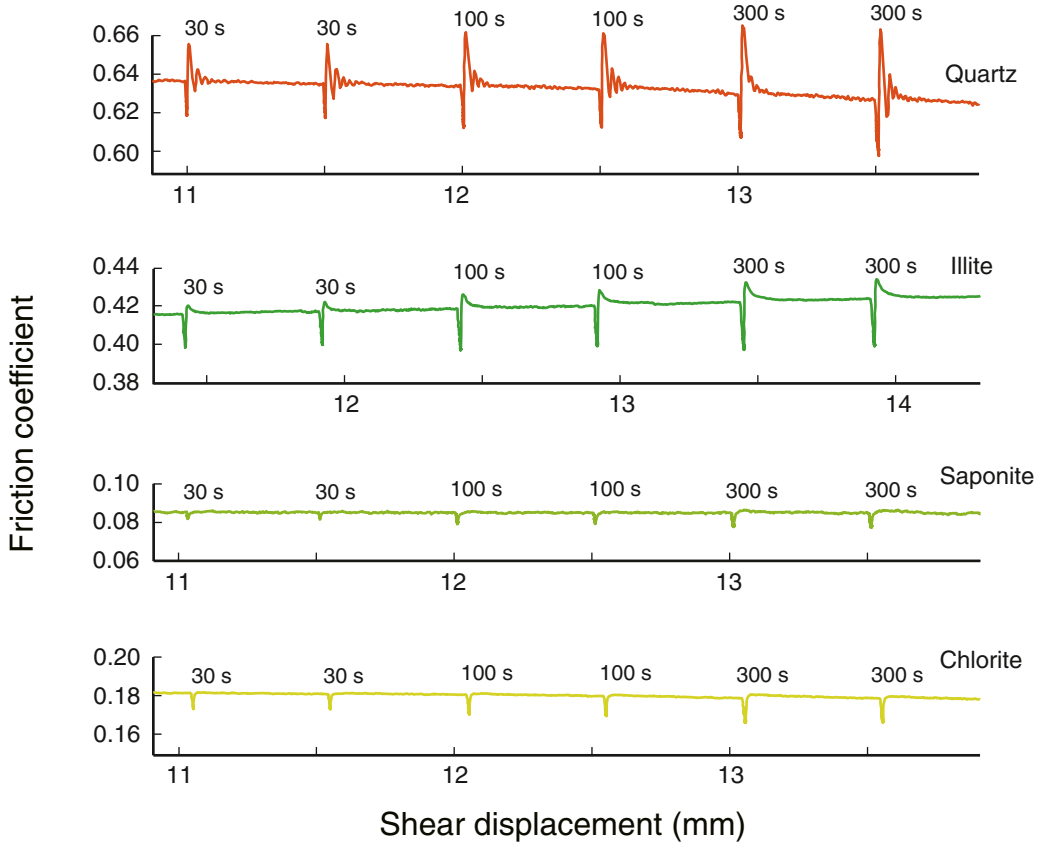

Fig. 3 Slide-hold-slide tests for each material under wet condition. The frictional healing ($\Delta\mu$) differs markedly between quartz and clay minerals, in which clay minerals show weak frictional healing

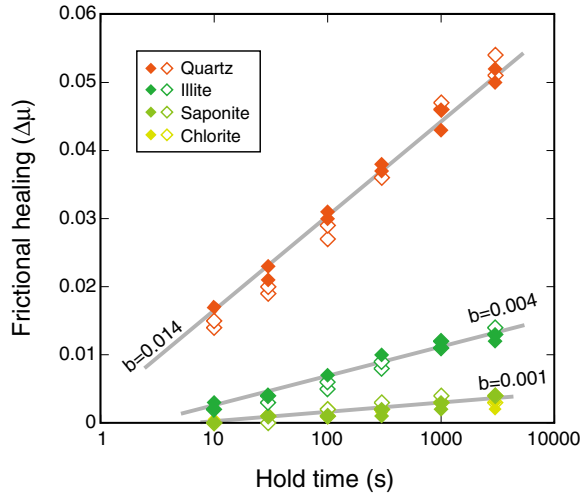

Fig. 4 Frictional healing ($\Delta\mu$) of clay minerals and quartz under wet conditions. Frictional healing systematically increases with holding time; however, clay minerals show a much lower healing rate than quartz. The *slopes* indicate healing rates of $b = 0.014$ for quartz, $b = 0.004$ for illite, and $b = 0.001$ for saponite and chlorite. The *filled symbols* indicate the experiments using pure water, and the *open symbols* indicate the experiments using 0.5 M NaCl water

The time-dependent healing of frictional strength is thought to result from changes in the contact area along a fault surface (Dietrich 1972). At the microscopic scale, it is the normal stress applied at a contacting asperity that represents the actual contact area on a fault surface, meaning that the local stress can be significantly higher than the macroscopic stress, resulting in creep at the point contact. The area of indentation has been observed to increase with the logarithm of time (e.g., Dieterich and Conrad 1984), and the evolution of contacting asperities has been directly observed in optically transparent materials (Dietrich and Kilgore 1994). This indicates that the observed difference in healing between quartz and clay minerals could be caused by the creep strength of clay minerals, in which clay minerals are characterized by a markedly small yielding stress, several orders of magnitude smaller than that of quartz (Shen et al. 2004). Although the weak creep strength of clay minerals means that their real contact area can easily increase over time, the shear stress needed to break the contact could be much smaller than that for quartz. The rapid growth of creeping asperities in clay-rich faults causes a near saturation in contact surface area after only a short period of time. This mechanism could explain the low healing rate in the simulated clay faults.

The healing tests of clay minerals are also characterized by the relatively large transient distance after peak to steady-state friction. The sliding of fault surface after stational holding results in the asperity contact of prior state to be removed, and the new population of contact reaches to a steady state after slip over a characteristic distance. This suggests that the transient distance from peak to steady-state frictions relates to the actual contact dimension (e.g., Scholz 2002). The relatively large slip-weakening distance found in clay minerals is therefore attributed to the extended real contact area.

As temperature increases along subduction, healing processes might be enhanced by thermally activated creeping, particularly under hydrothermal conditions. Nakatani and Scholz (2004) conducted experiments under hydrothermal conditions to examine the frictional healing of quartz. They showed that the frictional healing under hydrothermal conditions is controlled mainly by fluid-assisted solution transfer processes. Although the pressure solution creep is unlikely to operate in our room temperature experiments, it might be important for healing processes in natural fault zones.

Implications for the subducting plate interface

Clay minerals are frequently observed in the sediment layers of incoming plates into subduction zones and are commonly recognized in drill cores recovered from accretionary prisms (e.g., Underwood 2007). In the shallow part of a subduction zone, the plate boundary is poorly coupled due to the presence of unconsolidated sediments, meaning that earthquakes are rare in these regions. However, slip along the subducting plate can occasionally occur at close to the trench, which generates tsunami by seafloor displacement (e.g., Satake and Tanioka 1999). Although regions predominated by clay minerals cannot accumulate a large elastic strain, the frictional weakness of such layers might enhance the rupture propagation at shallow parts of subduction zones. In fact, the samples recovered from the Japan trench show a dynamic weakening during high-velocity rotary experiments, which can explain shallow slip and heat anomalies in the slip zone during the Tohoku-oki earthquake (Ujiie et al. 2013).

Along subduction zones, the layer of clay minerals becomes dehydrated as temperature increases (e.g., Moore and Vrolijk 1992), and this layer is also trapped by hanging-wall crust due to tectonic erosion (e.g., Hilde 1983). Seismic reflection surveys show that the decollement step-down to the top of the subducting oceanic basement in the Nankai accretionary wedge due to underplating of the sediment layer (Park et al. 2002). Consequently, it is possible that the hydration state of relatively deep plate boundaries and seismogenic zones is controlled mainly by fluid supply and migration from the subducting oceanic crust (e.g., Hyndman and Peacock 2003). Seismic velocities and attenuation beneath the forearc regions of northeast Japan indicate a highly heterogeneous fluid distribution along the plate boundary that may be spatially correlated with the occurrence of repeated large earthquakes (Zhao 2015).

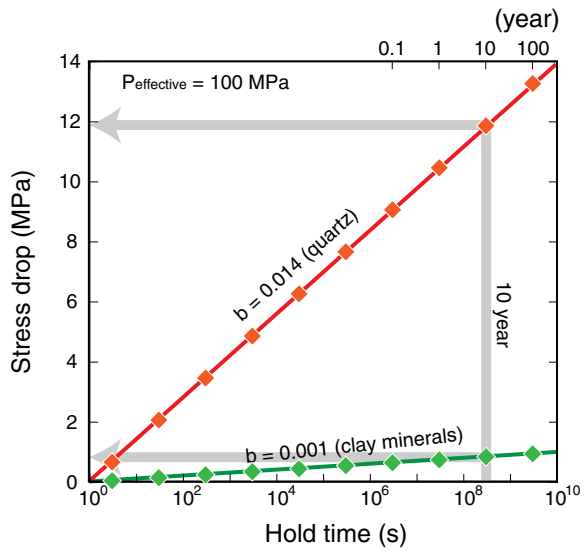

Fig. 5 Calculated stress drop as a function of hold time for regions dominated by quartz and clay minerals. In the calculation using experimentally determined healing rates equal to 0.014 for quartz and 0.001 for clay minerals, effective stress was assumed to be 100 MPa, and the stress accumulation yields 11.9 MPa for quartz and 0.8 MPa for clay minerals during an inter-seismic period of 10 years

Our experimental results indicated that the recovery of fault strength differs according to materials, in which clay minerals show weak and slow recovery. In the regions of extensively hydrated plate boundaries that produce abundant clay minerals such as chlorite, a large elastic strain is difficult to accumulate and does not generate large thrust earthquakes, whereas the regions escaped from the hydration reactions could result in a strong mechanical coupling that acts as a seismic asperity. The descending plate undergoes changes in mineralogy at certain pressures and temperatures; however, these mineralogical transformations cannot explain the lateral heterogeneity in coupling along the plate interface. The subduction of seamounts may explain such variations in coupling (Cloos 1992; Scholz and Small 1997). However, Wang and Bilek (2011) suggested that subducted seamounts are mostly aseismic and produce numerous small earthquakes, indicating that the regions containing subducted seamounts are unlikely to be locked; instead, they release strain energy by slip on complex fracture systems. This behavior is probably due to the relatively high permeability around seamounts inferred from heat flow data (Hutnak et al. 2008). Audet and Schwartz (2013) proposed that the spatial distribution of fluid supply is a consequence of the complex hydrological structure of oceanic crust and is related to the geometry of palaeospreading ridges. Irregularities in seafloor topography could also contribute to heterogeneity in fluid pathways along subduction interfaces. Hydration

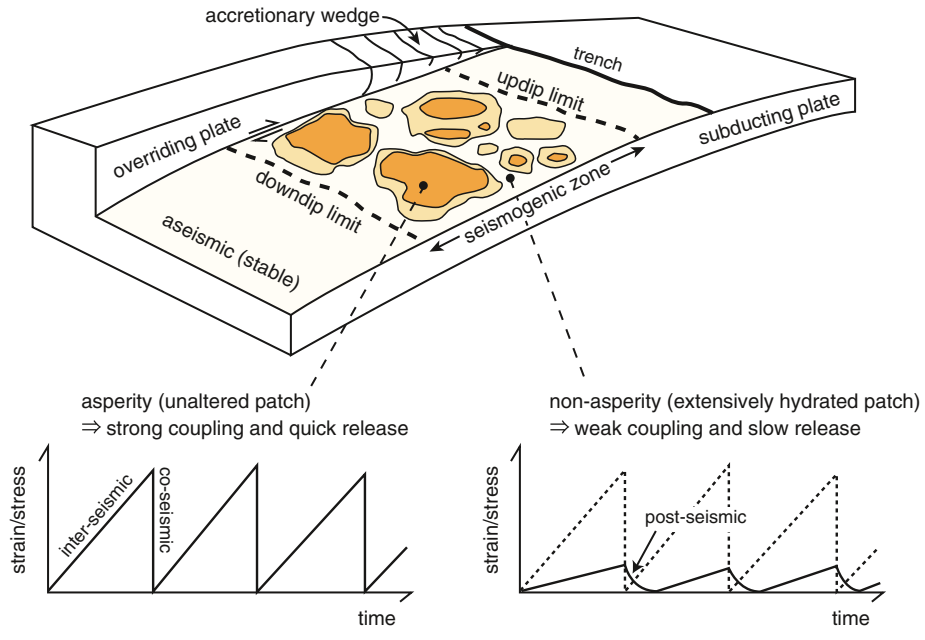

Fig. 6 Schematic model of the plate interface at a subduction zone (modified after Dixon and Moore 2007). Fluid supply to the plate interface promotes hydration reactions, forming clay minerals, which influence the frictional properties of the subducting plate. The clay-rich regions of the interface could be weakly coupled and act as non-asperity, whereas the unaltered patches remain strongly coupled and have the potential to generate megathrust earthquakes. Schematic model of the seismic cycle for subduction zone earthquakes, showing co-seismic slip generated by the unhydrated strongly coupled patches and post-seismic slip controlled by the weakly coupled hydrated patches

reactions result in a progressive change in mineralogy at the plate interface. The frictional properties of a fault zone depend on the amount of clay minerals, as friction coefficient decreases with increasing clay content (Tembe et al. 2010). Consequently, the boundary between extensively hydrated and unaltered regions may display a transitional behavior. Moreover, in addition to mineralogical variations, pore fluid pressure plays a key role in controlling the occurrence of slip at the subducting plate interface (e.g., Seno 2003).

We calculated the stress accumulation during an inter-seismic period using the experimentally determined healing rates. The results indicate 11.9 MPa for an altered patch and 0.8 MPa for a clay-rich patch, assuming an effective normal stress of 100 MPa and an inter-seismic time interval of 10 years (Fig. 5). Note that the seismologically determined stress drop is the average value for the entire slip patch and is not directly linked to our calculation. In any case, these results indicate that the stress accumulation during inter-seismic periods can differ substantially between unaltered and hydrated regions. When dynamic rupture occurs in unhydrated regions, the surrounding hydrated area also begins to slip; however, the rate of moment release is relatively low because of the large transient distance in clay-rich faults, which may control the rate of post-seismic slip after the main shock (Fig. 6). Global positioning system data have shown that the accumulated fault slip due to post-seismic movement is comparable to that released by the co-seismic event, but the rate of moment release is much lower than that of co-seismic rupture (Heki et al. 1997). The slow propagation of post-seismic events is simulated by fault properties with a large slip-weakening distance (Ariyoshi et al. 2007), which is consistent with the frictional properties of clay-rich faults.

In this study, we focused mainly on the recovery process of fault strength; however, the velocity dependence of friction is another important parameter that controls whether a fault has potential for seismic or aseismic slip. Velocity-weakening behavior is known to accelerate slip propagation that is potentially unstable and may cause a rupture to propagate, as opposed to the self-stabilizing behavior of velocity-strengthening materials (e.g., Scholz 1998). Most clay minerals exhibit velocity-strengthening behavior at room temperature (Saffer and Marone 2003; Ikari et al. 2007; Moore and Lockner 2007). However, complex behavior of velocity dependence of clay minerals has been reported at elevated temperatures, in which velocity-weakening behavior is found at intermediate temperatures for illite-rich gouges, whereas velocity-strengthening behavior occurs predominantly at lower and higher temperatures (den Hartog et al. 2012). Further experiments are needed to test whether such behaviors are common in other clay minerals.

Conclusions

In our experiments, the fault strength showed a strong dependence on mineralogy, suggesting the importance of mineralogy in controlling mechanical coupling of the subducting plate interface. Since phase transformations cannot explain the spatial distribution of earthquakes along subduction zone, fluid supply and the products of hydration reactions could be key factors controlling regional variations in seismic coupling. This possibility is supported by the observed patterns of seismic velocities and attenuation in subduction zones, which indicate a highly heterogeneous fluid distribution along the plate boundary (Zhao 2015). Recent advances in seismic imaging allow the detailed structure and fluid pressure along the subduction zone to be monitored (Kodaira et al. 2004; Tsuji et al. 2008), and such monitoring of fluid pressure and movement may further help to determine the strength of coupling at the subducting plate interface.

Additional file

Additional file 1: Supplementary information. Figure S1. Experimental assembly of the slide-hold-slide test using a biaxial machine at Hiroshima University. In the wet experiments, the sample assembly was filled by water in the water tank, in which water chemistry was controlled by either distilled pure water or 0.5 mol/L NaCl solution. A magnetic stirrer was used to achieve a homogeneous composition in the water tank. **Figure S2.** Results for wet experiments using 0.5 M NaCl water.

Competing interests

The authors' declared that they have no competing interest.

Authors' contributions

IK, HS, and KK planned the project, and IK and TK conducted the experiments. All authors discussed the results and implications. All authors read and approved the final manuscript.

Acknowledgements

We thank T. Shimamoto and K. Okazaki for technical advice and W. Tanikawa for the materials for the friction experiments. Comments by J. C. Moore and two anonymous reviewers helped to improve the manuscript. This study was supported by the Japan Society for the Promotion of Science and a Grant-in-Aid of Science Research on the Innovative Area of "Geofluids".

Author details

[1]Department of Earth and Planetary Systems Science, Hiroshima University, Higashihiroshima 739-8526, Japan. [2]Environment and Energy Materials Division, National Institute for Materials Science, Tsukuba 305-0044, Japan. [3]Department of Earth Science and Astronomy, University of Tokyo, Meguro 153-8902, Japan.

Received: 6 May 2015 Accepted: 2 October 2015
Published online: 09 October 2015

References

Ariyoshi K, Matsuzawa T, Hasegawa A (2007) The key frictional parameters controlling spatial variations in the speed of postseismic-slip propagation on a subduction plate boundary. Earth Planet Sci Lett 256:136–146. doi:10.1016/j.epsl.2007.01.019

Audet P, Schwartz SY (2013) Hydrologic control of forearc strength and seismicity in the Costa Rican subduction zone. Nat Geosci 6:852–855. doi:10.1038/ngeo1927

Beeler NM, Hickman SH, Wong T (2001) Earthquake stress drop and laboratory-inferred interseismic strength recovery. J Geophys Res 106:30701–30713. doi:10.1029/2000JB900242
Beroza GC, Ide S (2011) Slow earthquakes and non-volcanic tremor. Annu Rev Earth Planet Sci 39:271–296. doi:10.1146/annurev-earth-040809-152531
Carpenter BM, Marone C, Saffer DM (2011) Weakness of the San Andreas Fault revealed by samples from the active fault zone. Nat Geosci 4:251–254. doi:10.1038/ngeo1089
Cloos M (1992) Thrust-type subduction-zone earthquakes and seamount asperities: a physical model for seismic rupture. Geology 20:301–304. doi:10.1130/0091-7613
den Hartog SAM, Peach CJ, de Winter DAM, Spiers CJ, Shimamoto T (2012) Frictional properties of megathrust fault gouges at low sliding velocities: new data on effects of normal stress and temperature. J Struct Geol 38:156–171. doi:10.1016/j.jsg.2011.12.001
Dietrich JD (1972) Time-dependent friction in rocks. J Geophys Res 77:3690–3697. doi:10.1029/JB077i020p03690
Dieterich JH, Conrad G (1984) Effect of humidity on time- and velocity-dependent friction in rocks. J Geophys Res 89:4196–4202. doi:10.1029/JB089iB06p04196
Dietrich JH, Kilgore B (1994) Direct observation of frictional contacts: new insights for state-dependent properties. Pure Appl Geophysi 143:283–302. doi:10.1007/BF00874332
Dixon TH, Moore JC. The seismogenic zone of subduction thrust faults: introduction. The seismogenic zone of subduction thrust faults. In: Dixon T, Moore C, editors. New York: Columbia Univ. Press; 2007. p. 2–14.
Heki K, Miyazaki S, Tsuji H (1997) Silent fault slip following an interplate thrust earthquake at the Japan trench. Nature 586:595–598. doi:10.1038/386595a0
Hilde T (1983) Sediment subduction versus accretion around the pacific. Tectonophysics 99:381–397. doi:10.1016/0040-1951(83)90114-2
Hutnak M, Fisher AT, Harris R, Stein C, Wang K, Spenelli G, Schindler M, Villinger H, Silver E (2008) Large heat and fluid fluxes driven through mid-plate outcrops on ocean crust. Nat Geosci 1:611–614. doi:10.1038/ngeo264
Hyndman RD, Peacock SM (2003) Serpentinization of the forearc mantle. Earth Planet Sci Lett 212:417–432. doi:10.1016/S0012-821X(03)00263-2
Ikari MJ, Saffer DM, Marone C (2007) Effect of hydration state on the frictional properties of montmorillonite-based fault gouge. J Geophys Res 112:B06423. doi:10.1029/2006JB004748
Kanamori H (1986) Rupture process of subduction-zone earthquakes. Annu Rev Earth Planet Sci 14:293–322. doi:10.1146/annurev.ea.14.050186.001453
Katayama I, Iwata M, Okazaki K, Hirauchi K. Slow earthquakes associated with fault healing on a serpentinized plate interface. Sci Rep 2013; 3: doi:10.1038/srep01784.
Kameda J, Ujiie K, Yamaguchi A, Kimura G (2011) Smectite to chlorite conversion by frictional heating along a subduction thrust. Earth Planet Sci Lett 305:161–170. doi:10.1016/j.epsl.2011.02.051
Kodaira S, Iidaka T, Kato A, Park OA, Iwasaki T (2004) High pore fluid pressure may cause silent slip in the Nankai trough. Science 304:1295–1298. doi:10.1126/science.1096535
Lay T, Kanamori H, Ruff L (1981) The asperity model and the nature of large subduction zone earthquake occurrence. Earthquake Prediction Res 1:3–71
Marone C (1998) Laboratory-derived friction laws and their application to seismic faulting. Annu Rev Earth Planet Sci 26:643–696. doi:10.1146/annurev.earth.26.1.643
Moore JC, Vrolijk P (1992) Fluids in accretionary prisms. Rev Geophys 30:113–135. doi:10.1029/92RG00201
Moore DE, Lockner DA. Friction of the smectite clay montmorillonite. The Seismogenic Zone of Subduction Thrust Faults. In: Dixon T, Moore C, editors. New York: Columbia Univ. Press; 2007. p. 317–345.
Morrow CA, Moore DE, Lockner DA (2000) The effect of mineral bond strength and adsorbed water on fault gouge frictional strength. Geophys Res Lett 27:815–818. doi:10.1029/1999GL008401
Nakatani M, Scholz C (2004) Frictional healing of quartz gouge under hydrothermal conditions: 1. Experimental evidence for solution transfer healing mechanism. J Geophys Res 109:B07201. doi:10.1029/2001JB001522
Park J, Tsuru T, Takahashi N, Hori T, Kodaira S, Nakanishi A, Miura S, Kaneda Y (2002) A deep strong reflector in the Nankai accretionary wedge from multichannel seismic data: Implications for underplating and interseismic shear stress release. J Geophys Res 107:B42061. doi:10.1029/2001JB000262
Saffer DM, Marone C (2003) Comparison of smectite- and illite-rich gouge frictional properties: application to the updip limit of the seismogenic zone along subduction megathrusts. Earth Planet Sci Lett 215:219–235. doi:10.1016/S0012-821X(03)00424-2
Sakuma H (2013) Adhesion energy between mica surfaces: Implications for the frictional coefficient under dry and wet conditions. J Geophys Res 118:6066–6075. doi:10.1002/2013JB010550
Satake K, Tanioka Y (1999) Sources of tsunami and tsunamigenic earthquakes in subduction zones. Pure Appl Geophys 154:467–483. doi:10.1007/978-3-0348-8679-6_5
Scholz CH (1998) Earthquakes and friction laws. Nature 391:37–42. doi:10.1038/34097
Scholz CH (2002) The mechanics of earthquakes and faulting, 2nd edn. Cambridge Univ, Press, UK
Scholz CH, Small C (1997) The effect of sea-mount subduction on seismic coupling. Geology 25:487–490. doi:10.1130/0091
Seno T (2003) Fractal asperities, invasion of barriers, and interplate earthquakes. Earth Planets Space 55:649–665. doi:10.1186/BF03352472
Shen L, Phang Y, Chen L, Liu T, Zeng K (2004) Nanoindentation and morphological studies on nylon 66 nanocomposites. I. Effect of clay loading. Polymer 45:3341–3349. doi:10.1016/j.polymer.2004.03.036
Tembe S, Lockner DA, Wong T (2010) Effect of clay content and mineralogy on frictional sliding behavior of simulated gouges: binary and ternary mixtures of quartz, illite, and montmorillonite. J Geophys Res 115:B03416. doi:10.1029/2009JB006383
Tesei T, Collettini C, Carpenter BM, Viti C, Marone C (2012) Frictional strength and healing behavior of phyllosilicate-rich faults. J Geophys Res 117:B09402. doi:10.1029/2012JB009204
Tsuji T, Tokuyama H, Pisani PC, Moore G (2008) Effective stress and pore pressure in the Nankai accretionary prism off the Muroto Peninsula, southwestern Japan. J Geophys Res 113:B11401. doi:10.1029/2007JB005002
Ujiie K, Tanaka H, Saito T, Tsutsumi A, Mori JJ, Kameda J, et al (2013) Low coseismic shear stress on the Tohoku-oki megathrust determined from laboratory experiments. Science 342:1211–1214. doi:10.1126/science.1243485
Underwood MB. Sediment inputs to subduction zones: why lithostratigraphy and clay mineralogy matter. The seismogenic zone of subduction thrust faults. In: Dixon T, Moore C, editors. New York: Columbia Univ. Press; 2007. p. 42–85.
Wang K, Bilek SL (2011) Do subducting seamounts generate or stop large earthquakes? Geology 39:819–822. doi:10.1130/G31856.1
Zhao D (2015) The 2011 Tohoku earthquake (Mw 9.0) sequence and subduction dynamics in Western Pacific and East Asia. J Asian Earth Sci 98:26–49. doi:10.1016/j.jseaes.2014.10.022